

# Pair-Symmetric and Pion Backgrounds for EG1b

P. Bosted

*University of Massachusetts, Amherst, MA 01003*

## Abstract

The fraction and double-spin asymmetry of detected electrons originating from pair-symmetric process is determined from a study of positron events. The fraction is found to be significant ( $> 10\%$ ) for  $E' < 0.4$  (1.0) GeV for incident beam energies of 1.6 (5.7) GeV. The asymmetry is found to be small compared to that for electrons, in most cases. Some of the events identified as positrons or electrons are in actuality mis-identified pions. For standard particle identification cuts, the fraction of electrons that are really pions can be as high as 5%. The asymmetry for positive and negative pions is found to generally be of the same order of magnitude as for electrons. Significant structure is seen in the 1.6 GeV data. Tables of correction factors are provided, and a suggestion is made for how to account for the combined pair-symmetric and pion backgrounds, and how to estimate the systematic error on the correction.

## 1 Introduction

There are two principal backgrounds to electron rates measured in Eg1b. This affect the measured asymmetries, and corrections must be made of the form:

$$A_{corr} = A_{raw} \frac{1 - \sum_i f_i (A_i/A_{raw})}{1 - \sum_i f_i},$$

where  $f_i$  are the fractions of events coming from a given background, and  $A_i$  is the raw asymmetry for each process. In the limit that  $A_i/A_{raw} \approx 0$ , the background is equivalent to a simple dilution. If  $A_i$  is equal to  $A_{raw}$ , then  $A_{raw}$  is actually unchanged, but the error is increased by  $1/(1 - \sum_i f_i)$ .

The first major background comes from secondary electrons (as opposed to primary beam electrons that made a single hard scattering from the target). The first source of secondary electrons is from wide-angle  $e^+/e^-$  pair production from bremsstrahlung photons generated in the target. The formulas for this process were worked out by Tsai [1]. The rates depend on knowing the form factors for elastic, quasi-elastic, and inelastic electron scattering. Because this process is very similar to the radiation of real photons in electron scattering (but in the pair production case, both leptons are in the final state, instead of

one in the initial, and one in the final state), the formulas are very similar to the usual Mo-Tsai radiative correction formulas, and the same form factors are needed. This process is also referred to as the Bethe-Heitler process, and for convenience I will label it “BH”. The leptons from BH are very forward peaked (characteristic angle  $m_e/E = 1/\gamma$ ), so the BH process is only significant at the most forward angles in CLAS.

The most important source of pair-symmetric leptons is from hadron decay, and especially  $\pi^0 \rightarrow e^+e^-\gamma$  (also known as the Dalitz decay), which has a branching ratio of 1.2%. The Dalitz decay probability is effectively enhanced in a thick target by the probability that one of the photons from the 99% probability  $\pi^0 \rightarrow \gamma\gamma$  pair produces at a small angle as it leaves the target. The enhancement is proportional to the average amount of material the photons pass through (in radiation lengths), scaled by a factor of two for the two photons. In Eg1b, the average photon passes through about 0.01 r.l. as it leaves the target, and roughly 0.005 r.l. in the front part of the region I drift chambers. If a conversion takes place beyond this point, there will not be enough hits for the secondary lepton to be registered as track. Thus, the effective Dalitz decay probability for  $\pi^0$ s is about 4%. The other main pseudoscalar particle, the  $\eta$ , can also generate lepton pairs from its Dalitz decay (0.6%), two-photon decay (40%), and  $3\pi^0$  decay (32%), but the overall importance is small due to the small average ratio of  $\eta/\pi^0$  in photoproduction.

Other sources of secondary leptons are from decays of the vector mesons  $\rho$ ,  $\omega$ , and  $\phi$  to  $e^+e^-$ . However, their decay probabilities are so small  $< 10^{-4}$  that they aren’t major contributors. This was checked using the photoproduction code PYTHIA [2] run with 5 GeV photons.

One source of leptons from hadron decays is not pair-symmetric, namely the 5% probability for  $K_L^\pm$  to decay to  $\pi^0 e^\pm \nu_e$ , because the typical ratio of  $K^+$  to  $K^-$  is about 2 to 4 in 2-5 GeV photoproduction. Fortunately, the great majority of kaons decay beyond the region I chambers, so combined with the small kaon to  $\pi^0$  ratio, this contribution is very small and can be neglected.

In summary, the principal source of secondary electrons is from the pair-symmetric decay of  $\pi^0$ s.

The second major background comes from  $\pi^-$  that pass the electron PID cuts. In Eg1b, a tradeoff in purity versus efficiency was made to minimize the final statistical error for the average kinematic bin. Higher cuts on the Cherenkov counter and calorimeter signals results in much lower pion contamination, at the expense of a substantial loss in electron efficiency.

## 2 $e^+/e^-$ Ratio

The factor  $f$  for the fraction of electrons coming from secondary processes was determined by analyzing runs taken with identical beam energies, but opposite torus polarity. In this way, the detector acceptance cancels in the measured ratio  $r_{in}$  of rates of positrons with negative torus polarity to electrons with positive torus polarity, and similarly for  $r_{out}$  of rates of positrons with positive torus polarity to electrons with negative torus polarity. The rates were determined using the ratio of events passing the standard Eg1b electron

cuts, divided by the live-time corrected Faraday cup readings. A loop was made over all particles for each trigger, and all particles passing the electron PID cuts were counted, so that a given trigger could include more than electron or more than one positron. A given trigger could include both electrons and positrons. In the Eg1b dst files, events with no negative tracks were stored in separate files (so-called “positron” files). Since there was not always as “positron” file for each “electron” file, the rates for each file type were formed separately then added to obtain the total rate.

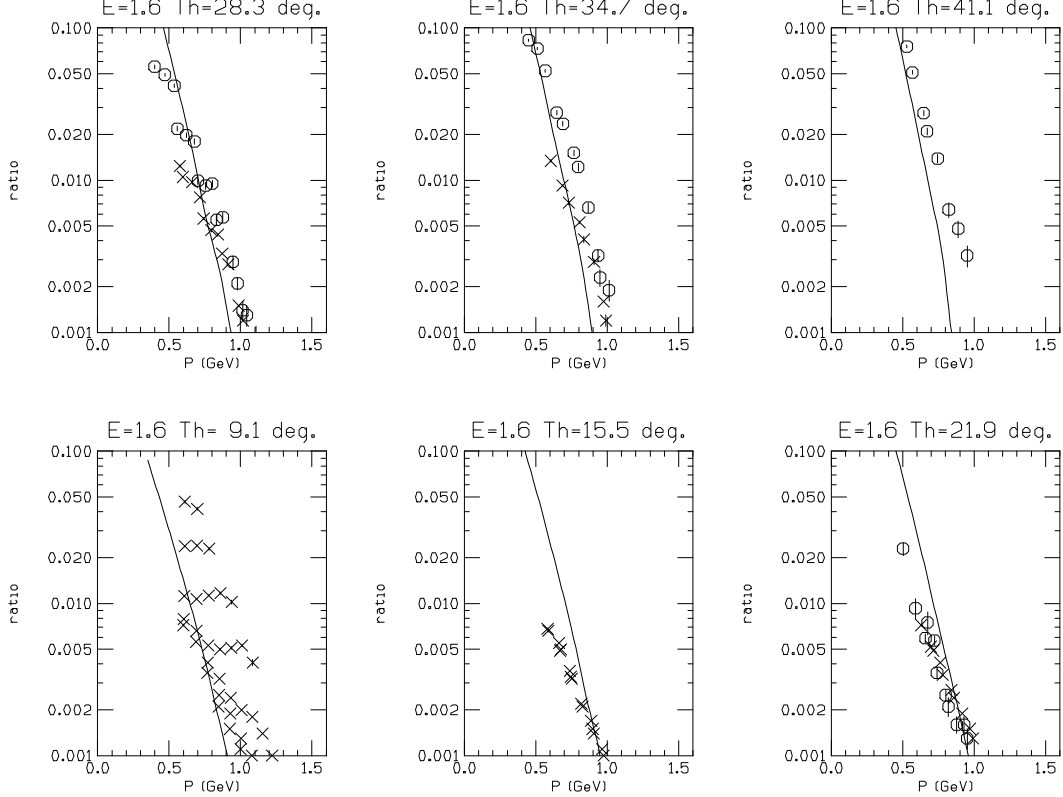


Figure 1: Measured rates of  $e^+/e^-$  for  $E = 1.6$  GeV for both particles in-bending ( $r_{in}$ , circles) and both particles out-bending ( $r_{out}$ , crosses), as a function of lepton momentum  $E'$ , for six scattering angles. The curves are from the model described in the text.

The ratios  $r_{in}$  (circles) and  $r_{out}$  (crosses) are shown at six scattering angles as a function of lepton momentum  $E'$  for the NH3 target in Fig. 1 for beam energy  $E = 1.6$  GeV and in Fig. 2 for  $E = 5.7$  GeV. The ratios for the ND3 target are almost identical (not shown). The ratios rise steeply with decreasing  $E'$ , exceeding about 10% for  $E' < 0.4$  GeV ( $E' < 1.2$  GeV) for  $E = 1.6$  ( $E = 5.7$ ) GeV. The ratios  $r_{in}$  and  $r_{out}$  are in reasonably good agreement, as they should be for cleanly identified leptons originating from the target, for 1.6 GeV at  $\theta < 25$  degrees, and for most of the 5.7 GeV data. However,  $r_{in}$  tends to be larger than  $r_{out}$ , especially for large angles at 1.6 GeV. This might be partially explained by the trigger and acceptance biases, allowing more than one electron or positron per trigger, changes in the calorimeter gain and trigger threshold (for  $E = 1.6$  GeV) and the difference in accidental

rates for the two torus polarities, which used different beam currents. Since it is hard to account for all of these factors, the difference between  $r_{in}$  and  $r_{out}$  should probably be treated as a reasonable estimate of the systematic error on the average ratio. For this reason, I estimate an overall systematic error of 0.3 on  $df/f$  (see section on systematic errors below).

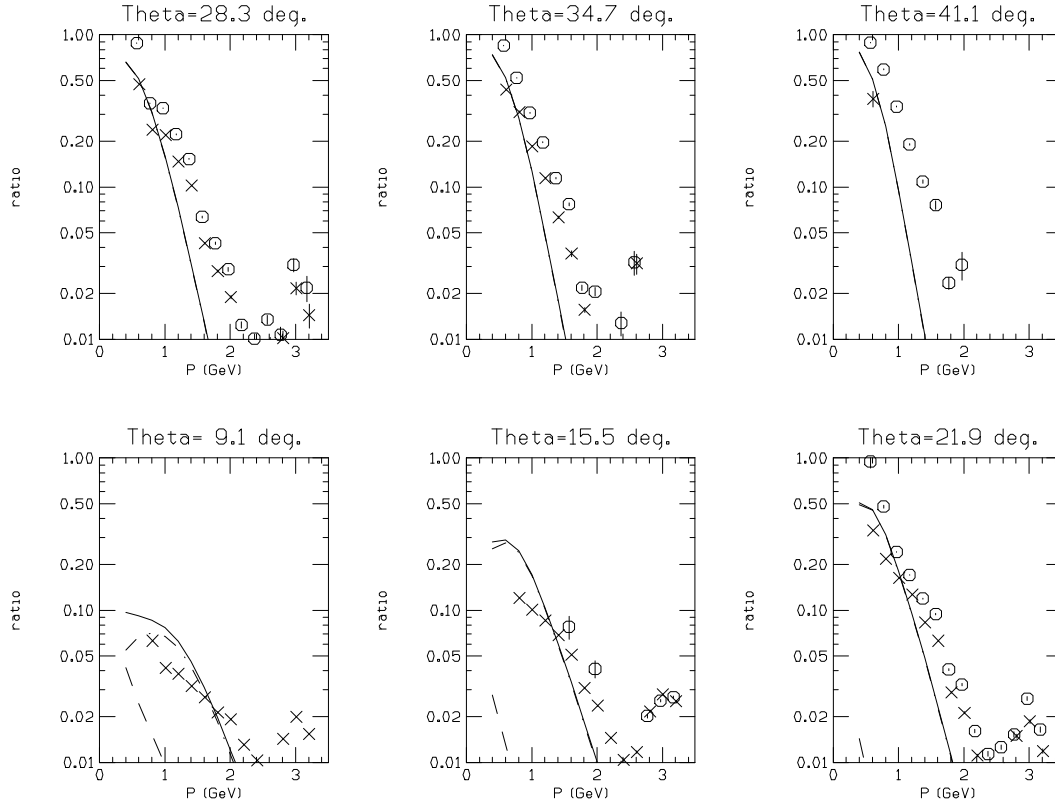


Figure 2: Same as Fig. 1 except for  $E = 5.7$  GeV.

The data in Figures 1 and 2 are compared to a model calculation, shown as the solid curves. The model used the Wiser fit [3] to  $\pi^+$  and  $\pi^-$  photoproduction yields, (normalized by half the target thickness of 0.009 r.l. plus an effective radiator thickness of 0.025 to account for small-angle electroproduction), to predict the rate of  $\pi^0$  production (taken as the average of  $\pi^+$  and  $\pi^-$  rates). This model was checked against the Lund Monte Carlo code PYTHIA [2] and found to agree within 30% or so. Photons from the  $\pi^0$  decays were converted to  $e^+/e^-$  pairs evenly distributed in energy, collinear with the photon direction, according to a conversion probability of 0.008 (the average amount of material traversed by the photons in r.l. times 7/9). Dalitz decays were treated by enhancing this probability by 0.006 (half the Dalitz branching ratio since twice as many photons in  $\pi^0 \rightarrow \gamma\gamma$  as in  $\pi^0 \rightarrow e^+e^-\gamma$ ). The primary electron rate was calculated using the Mo-Tsai radiative correction code [1] to predict radiated cross sections [except at  $E = 1.6$  GeV where Born cross sections were used]. It can be seen that the predictions are generally in reasonable agreement with the observed ratios, within the expected model uncertainty of about 30%,

except at high  $E'$ . The excess for  $E' > 2.7$  GeV for  $E = 5.7$  GeV is entirely due to pions which are mis-identified as electrons, because 2.7 GeV is the Cherenkov threshold in Eg1b, and above this momentum only the calorimeter can be used for electron/pion separation. This is illustrated in Fig. 3, where the left panel shows the standard electron definition, and the right panel shows the results using a definition requiring  $E_{tot}/P > 0.27$  and  $C_{cer} > 4$ , where  $E_{tot}$  is the total calorimeter signal,  $p$  is the particle momentum, and  $C_{cer}$  is the Cherenkov signal in units of photoelectrons. [The standard definition at 5.7 GeV used  $E_{tot}/P > 0.20$  and  $C_{cer} > 2.5$  for  $P < 3$  GeV and  $E_{tot}/P > 0.24$  and  $C_{cer} > 0.5$  for  $P > 3$  GeV]. Note that the agreement with the model is improved with the tight electron cut at high  $E'$  and also at high  $Q^2$ .

Calculations were also made of the Bethe-Heitler contributions to the positron spectra. They were found to be negligible except at  $\theta < 10$  degrees, and even at 6 degrees the  $\pi^0$  contribution is still dominant.

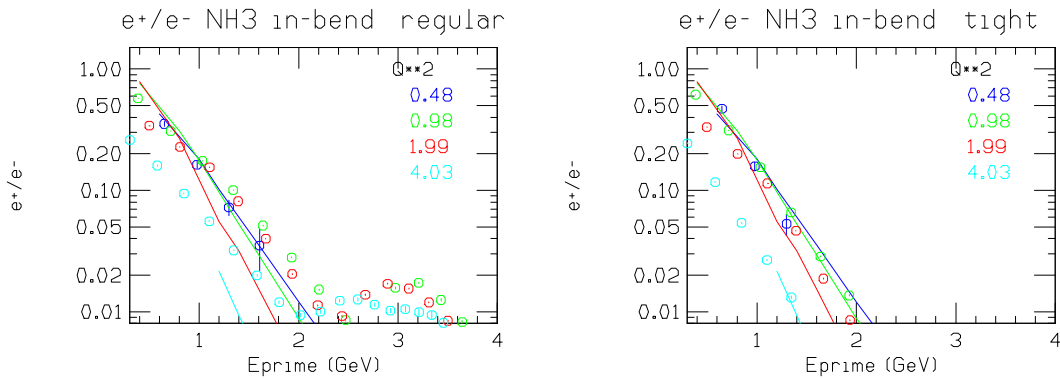


Figure 3: Ratios  $r_{in}$  for various bins in  $Q^2$  for  $E = 5.7$  GeV for the regular electron definition (left) and a tight definition that greatly reduces pion contamination (right).

### 3 Studies of pion contamination

To make more detailed studies of the relative rates of pions in the electron and positron spectra, histograms of the  $E/P$  spectrum were stored for each run for both positive and negative particles, and three particle ID definitions. The ratio of calorimeter energy  $E$  to particle momentum  $P$  was scaled by  $1/0.27$  so that the peak for electrons should be near 1 (or 1.1 for runs where the calorimeter was calibrated using a constant of 0.3 instead of 0.27). The three definitions were: 1) Cherenkov signal  $C_{cer} > 2.5$ ; 2)  $0.3 < C_{cer} < 1.5$ ; 3)  $C_{cer} > 5$ . All definitions also used standard vertex and fiducial acceptance cuts, and in addition required  $\beta$  within 0.03 of unity to remove protons and kaons. The study was only done up to  $P = 2.7$  GeV, because above that momentum the Cherenkov is no longer a good discriminant between pions and electrons. Definition 1 essentially corresponds to the standard electron PID cuts (without the  $E/P$  cut), definition 2 to mostly pions, and definition 3 to mostly electrons. The definition 1 spectra were then fitted with two

parameters: an electron shape (defined using negative particles and definition 3) and a pion shape (defined using positive particles and definition 2). These two-parameter fits generally gave quite a good description of the definition 1 spectra for both positive and negative particles, as shown in Fig. 4 for a typical momentum and angle at both  $E = 1.6$  and  $E = 5.7$  GeV.

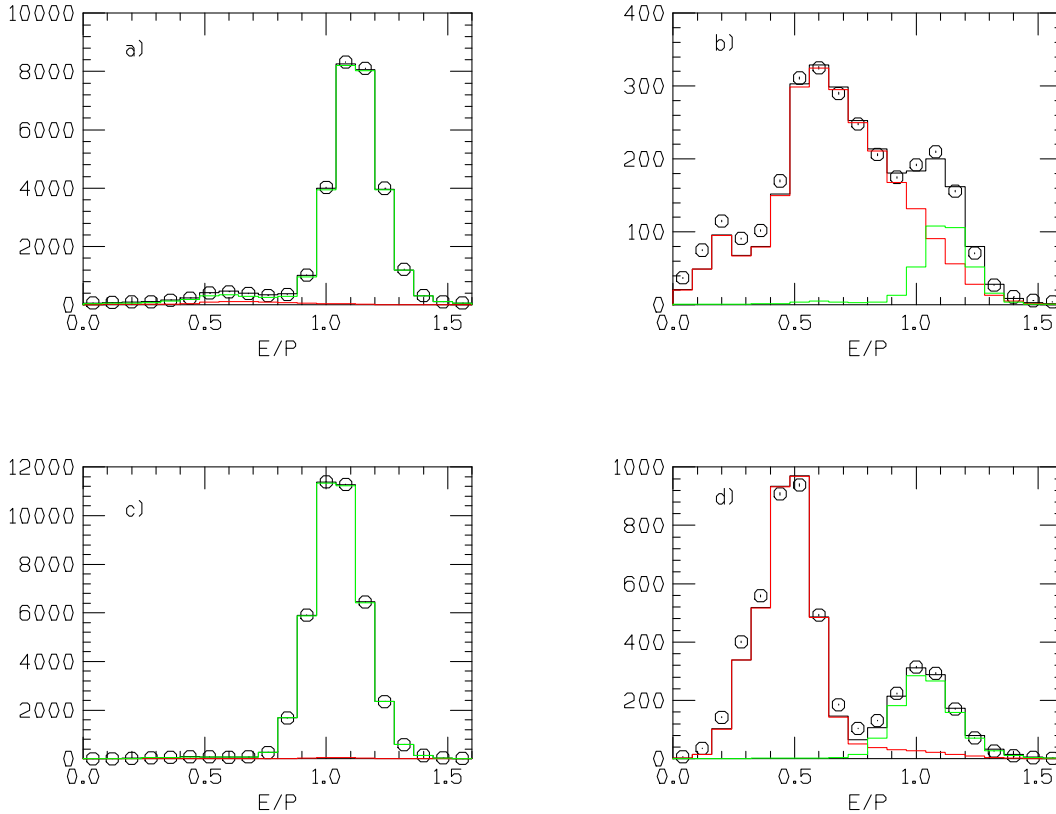


Figure 4: Normalized calorimeter energy spectra for a) negative and b) positive particles for  $E = 5.7$  GeV,  $P = 1.7$  GeV, and  $\theta = 13.5$  degrees. The red curve on the left and the green curve on the right of each panel were fit to the total spectrum. The red curve was obtained from a sample of “pure” pions, and the right curve for “pure” electrons. Spectra for  $E = 1.6$  GeV are shown for  $P = 1$  GeV and  $\theta = 13.5$  degrees for c) negative and d) positive particles. Essentially no pions are visible in c).

Note that the “pion” shapes are cut off at low  $P$  due to the trigger thresholds for the inner and total calorimeter signals: ideally an unbiased, low threshold trigger would have been available, but trigger 7 (prescaled by 50) had the same two EC thresholds as the electron trigger, and trigger 8 (prescaled by 100 to 400), had the same total energy requirement, although with no requirement on the inner layer signal. This probably accounts for the two-component look to the “pion” spectra”.

Ratios of  $e^+/e^-$  from rates of “pure” electrons and positrons from the above-mentioned fits were calculated, and representative results for  $E = 5.7$  GeV are shown in Fig. 5. The results are fairly similar to those using the “tight” electron cuts described earlier, and are

in reasonable agreement with the model. There is somewhat better agreement between outbending and inbending ratio.

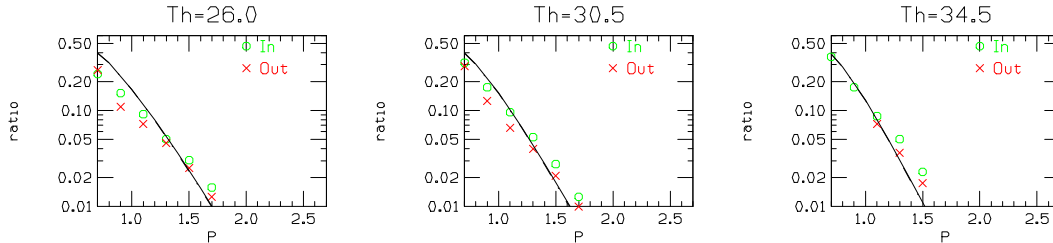


Figure 5: Ratio of “pure”  $e^+$  to  $e^-$  from analysis of  $E/P$  spectra (as shown in Fig. 4) for  $E = 5.7$  GeV and for leptons both inbending or both outbending. The curve is the model as in Fig. 2 and Fig. 3.

Of more interest perhaps is that this fitting method can also give the fraction of standard PID electrons that are actually mis-identified pions (below 2.7 GeV). The results are shown in Fig. 6 for  $E = 5.7$  GeV at nine angles. The inbending and outbending ratios are in excellent agreement, and show an approximately exponential decrease from about 0.05 at  $P = 1$  GeV to  $< 0.01$  for  $P > 2$  GeV. Comparing to the  $e^+/e^-$  ratios shown in Fig. 2 for the standard electron PID, one can see that about 1/3 of the ratio is coming from mis-identified pions, and about 2/3 from true positrons. Above 2.7 GeV, the ratios would rise again, as shown in Fig. 2, to typical values of 0.02, for equal rates of  $\pi^-$  and  $\pi^+$ . This is because the “positron” spectrum in Fig. 2 contains no actual positrons above 2.7 GeV: the counts are all due to mis-identified pions.

Another ratio of interest is that of  $\pi^-$  to  $\pi^+$ . This was examined using a “pion” definition that required that the particle be the “trigger” particle (as defined in the off-line analysis) and that  $E/P$  be below the cut used for electrons. It is not a great definition, especially as positive and negative pions don’t deposit the same amount of energy on average in the calorimeter, but given that there was no really good hadron trigger (triggers 7 and 8 had quite high calorimeter thresholds with low pion efficiency), this is the best I could think of. The ratios of yields are shown in Fig. 7 for both particles inbending (left), or both outbending (right), for various bins in  $Q^2$ . The ratios are between 1 and 2 at low  $Q^2$  (which account for the vast majority of triggers), increasing to as high as 5 at high  $Q^2$ . An alternate pion definition that also required a Cherenkov signal less than 2.5 p.e. shows similar behavior. While the results are not particularly trustworthy, they do indicate that in all cases that the inverse ratio, that of  $\pi^-/\pi^+$ , is less than unity. This means that using the  $e^+/e^-$  ratios defined with the standard electron PID (as in Fig. 2), probably overestimates the total contribution of pions, and are unlikely to be too large if used to estimate the total rate of secondary electron and mis-identified  $\pi^-$ .

For the  $E = 1.6$  GeV, pions are much less of a concern than at 5.7 GeV because the pion yields change slowly (approximately as  $\ln(E)$ , while the electron cross section varies as at least  $1/E^2$ ). Studies of the  $E/P$  spectra show little evidence for pions when a Cherenkov signal is required.

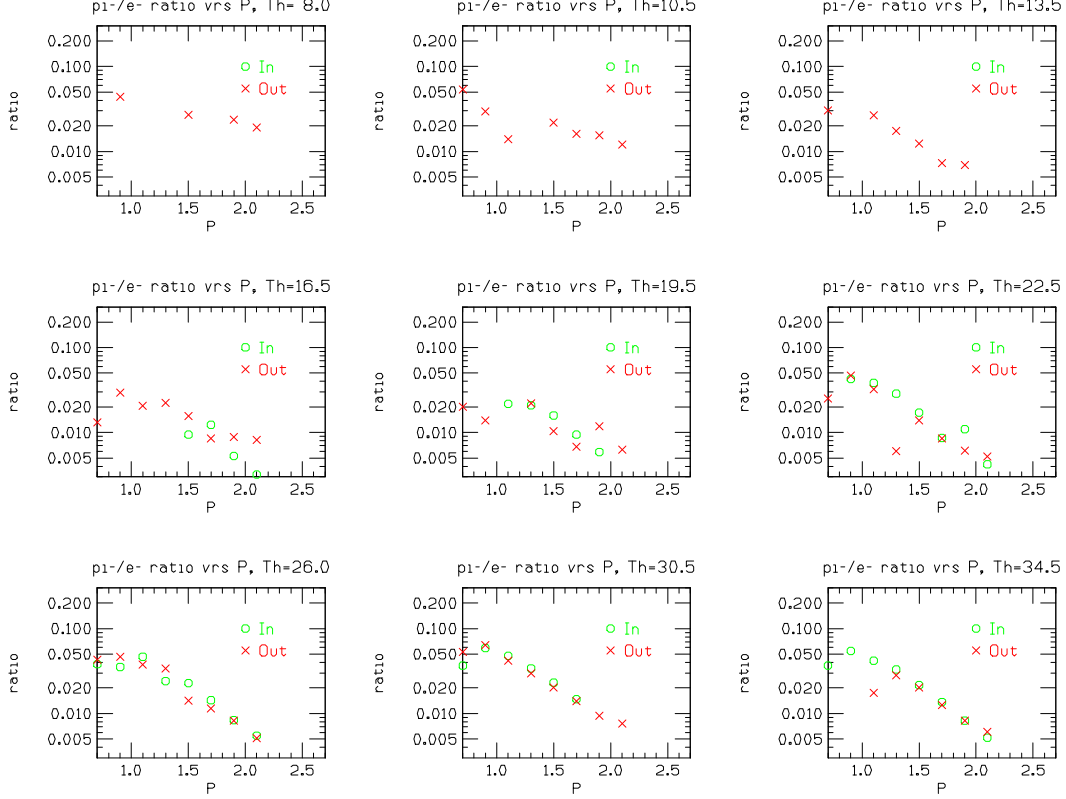


Figure 6: Ratio of “pure”  $\pi^-$  to  $e^-$  from analysis of  $E/P$  spectra (as shown in Fig. 4) for  $E = 5.7$  GeV and for particles both inbending or both outbending. No fits were done above 2.7 GeV.

## 4 Positron and pion asymmetries

As mentioned in the introduction, both the rate and asymmetry of background processes are needed to correct the measured inclusive electron asymmetries. What is important is the ratio of the background asymmetry to the primary electron asymmetry, scaled by the relative rate of the background process.

To first order, the background from both secondary leptons and pions can be studied using positrons that pass the standard electron PID cuts. The asymmetry will be dominated by pair-symmetric events, except at high  $E$  and  $E'$ , where pions become increasingly important. The asymmetry for positive and negative particles satisfying the standard PID cuts is shown in Fig. 8 for  $E = 1.6$  GeV and in Fig. 9 for  $E = 5.7$  GeV. To obtain adequate statistics, the events have been averaged over  $Q^2$ . An addition cut  $E' > 0.5$  (0.85 GeV) has been applied for the  $E = 1.6$  GeV (5.7 GeV) data to roughly match cuts that will be used for the final physics analysis (although the results are not changed much compared to having no cuts).

The “ $e^+$ ” asymmetries are generally close to zero, compared to the  $e^-$  asymmetries, at most of the kinematics of eg1b. For the  $E = 1.6$  NH3 data, the statistical errors are



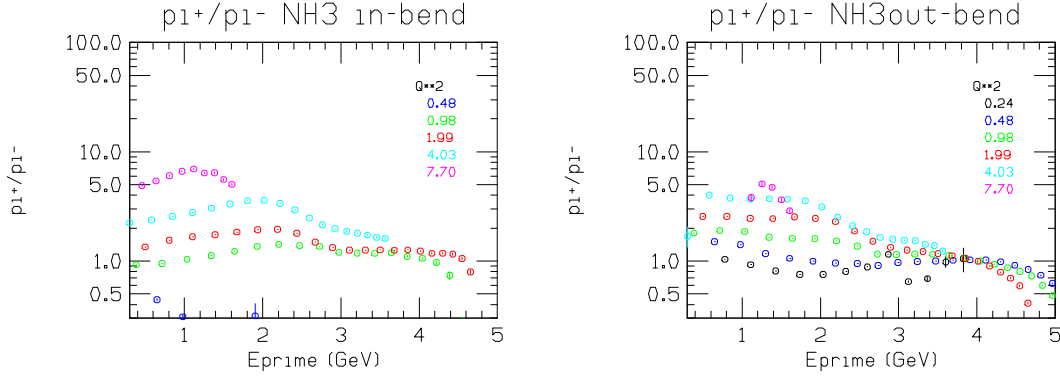


Figure 7: Ratio of  $\pi^+$  to  $\pi^-$  for both particles inbending (left) and both particles outbending (right), for various bins in  $Q^2$ , for  $E = 5.7$  GeV.

relatively large (due to the relatively small value of  $f$ ), so the ratio of background to electron asymmetries can roughly speaking be described as being somewhere between -1 and 1. For the  $E = 5.7$  NH3 inbending data, the absolute value of the ratio is generally less than 0.1, so the background can be treated as a pure dilution to quite good accuracy. For the outbending case, the ratio is generally less than 0.2, although there is a tendency for the ratio to approach 1 at high  $W$ . In the case of ND3, the  $e^-$  asymmetries are much smaller than for NH3, so the ratio of background to electron asymmetries can be larger. Within the limited statistical errors, the ratio is consistent with being between -1 and 1.

The double-spin asymmetries for positive and particles passing the loose “pion” cuts described above (and used for the ratios shown in Fig. 7) are compared with the electron asymmetries in Fig. 10 for  $E = 1.6$  GeV and Fig. 11 for  $E = 5.7$  GeV. For the 1.6 GeV data, the NH3 asymmetries are of the same order as the electron asymmetries, for both signs. For the ND3 target, a rather interesting result is seen: the  $\pi^-$  asymmetries are strongly negative at low  $W$ . This is perhaps not too surprising: low  $W$  corresponds to high  $P$ , hence to photon energies near 1.6 GeV if the pions originate from quasi-real electroproduction. The highest energy photons are the most polarized, and the  $\pi^-$  asymmetry is known to be strongly negative in this energy range. Fortunately, the fraction of pions mis-identified as electrons is small in this  $W$  region, so the contamination to the electron asymmetry is hopefully small also. However, this region deserves special care.

For the 5.7 GeV, the pion asymmetries are generally less than 20% in magnitude compared to the NH3 electron asymmetries. The pion asymmetries for ND3 tend to all be negative, and are on average about half the magnitude of the electron asymmetries. For all the 5.7 GeV, the pion asymmetries are consistent with the “positron” asymmetries, so can be treated on an equal footing in considering the systematic error in the background corrections.

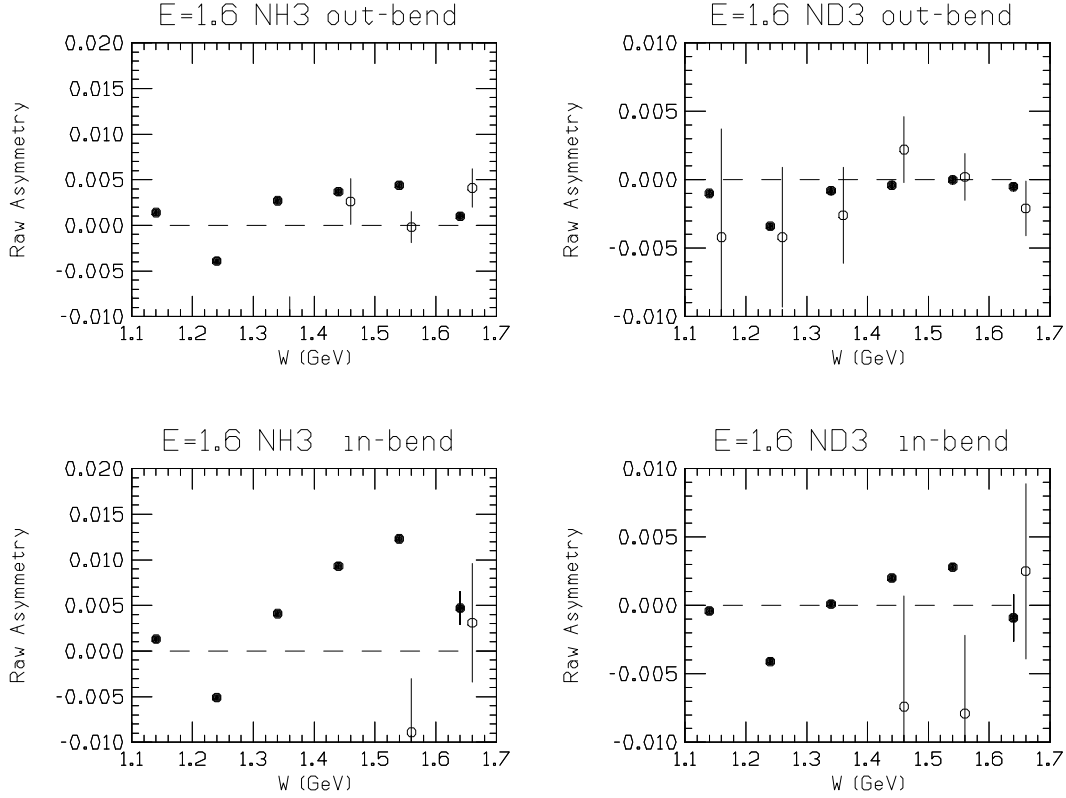


Figure 8: Raw double-spin asymmetries for the indicated targets for inbending and out-bending polarities of the torus, for  $E = 1.6$  GeV. The data are averaged over  $Q^2$  and plotted as a function of  $W$ . The solid circles are for negative particles passing the standard electron PID cuts, and the open circles are for positive particles passing the same cuts.

## 5 Systematic error in background correction

It is possible to rewrite Eq. 1 in terms of a dilution factor only, assuming that the background asymmetry is zero, but has an uncertainty given by  $dA_b/A_e$ . We lump all the background into a single dilution factor  $f$ , which can be done by defining  $f$  as the ratio of “positrons” to “electrons” with standard PID cuts, and assuming that the  $\pi^-/\pi^+$  ratio is or order 1 or less (as supported by the data). In this case:

$$A_{corr} = A_{raw}/1 - f$$

and the systematic error is given by

$$dA_{corr} = A_{raw} \sqrt{(df)^2 + [f(dA_b/A_e)]^2}$$

Given the discussion in the previous sections, reasonable guesses for the two parameters  $df$  and  $dA_b/A_e$  are listed in Table I for the two beam energies, torus polarities and targets of Eg1b so far analyzed.

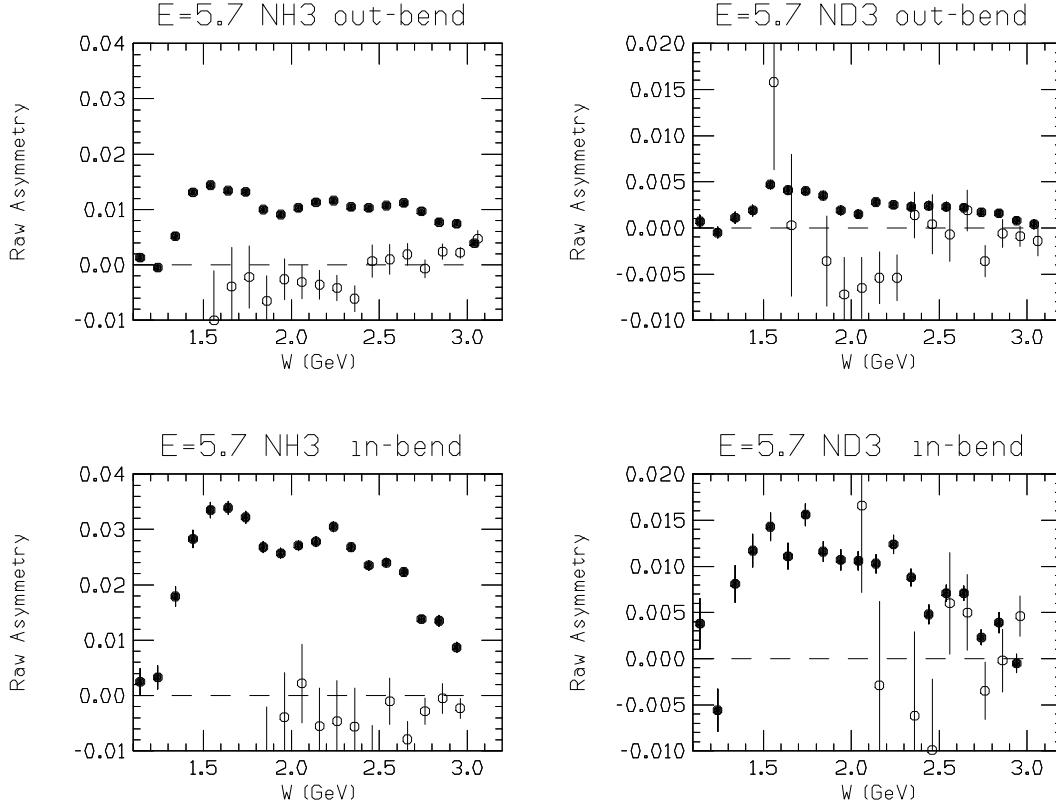


Figure 9: Same as Fig. 8, but for  $E = 5.7$  GeV.

## 6 Location of tables, plots, and tex source

All files are located in <http://www.jlab.org/Hall-B/secure/eg1/EG2000/Bosted/background/>. The positron/electron ratios for standard electron PID are listed in the files posratXY.dat, where X is 16 for 1.6 GeV and 57 for 5.7 GeV, and Y is p for NH3, and d for ND3. The file readme.txt gives details of how to use these files. There is also a file called pasrat.dat, which has the ratios for a “tight” electron definition for NH3 (results almost identical for ND3). The source for the present document is eg1bbknd.tex, and the figures can be found in eg1bbknd.pltX (for the topdraw input files, containing the plotted values in ascii format), and eg1bbknd.figX (for the postscript files), where X is a figure number from 1 to 11. The computer code to calculate the pair-symmetric contributions from  $\pi^0$  decays is called pi0.f, and the Bethe-Heitler code is called bhs.f. Comments in the codes explain how to use them. The code to calculate radiated electron cross sections is not included, as such codes are widely available elsewhere.

## References

- [1] Y. S. Tsai, Rev. Mod. Phys. 46 (1974) 815.

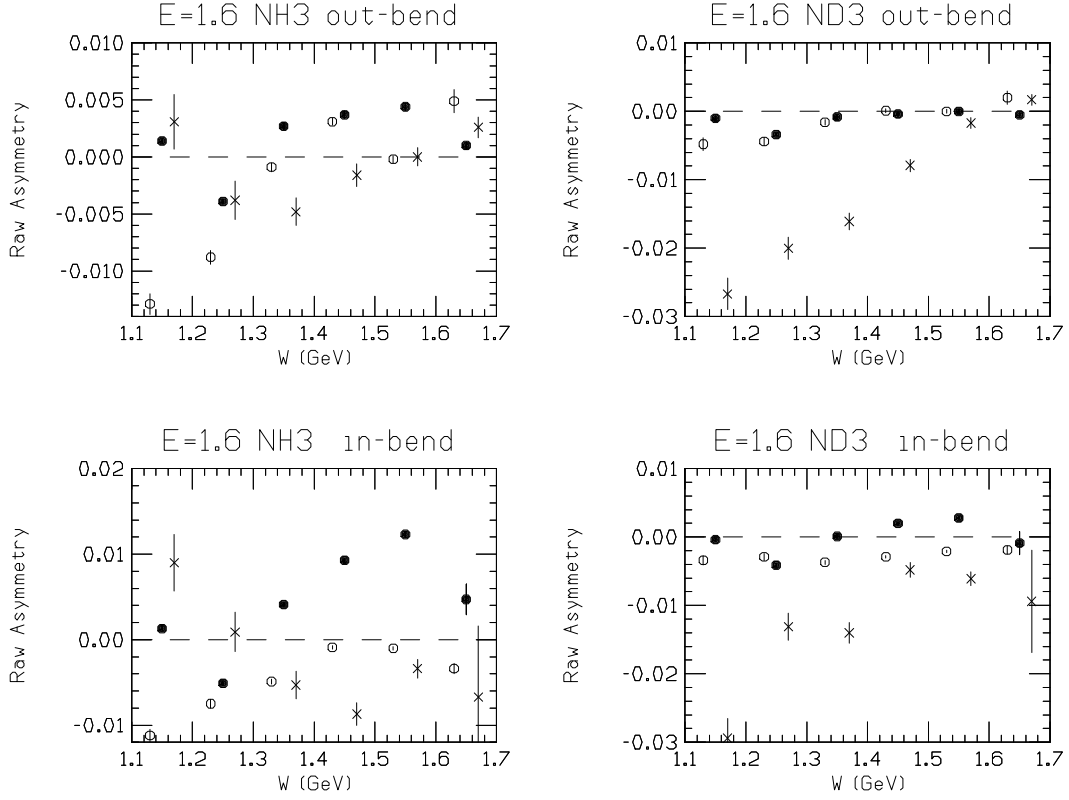


Figure 10: Raw double-spin asymmetries for the indicated targets for inbending and outbending polarities of the torus, for  $E = 1.6$  GeV. The data are averaged over  $Q^2$  and plotted as a function of  $W$ . The solid circles are for negative particles passing the standard electron PID cuts, while the open circles are for positive particles passing loose “pion” cuts, and the crosses are for negative particles passing the same pion cuts.

[2] T. Sjostrand, Computer Physics Commun. 82, 74 (1994).

[3] D.E. Wiser, Ph.D thesis, U. of Wisconsin, 1977 (unpublished).

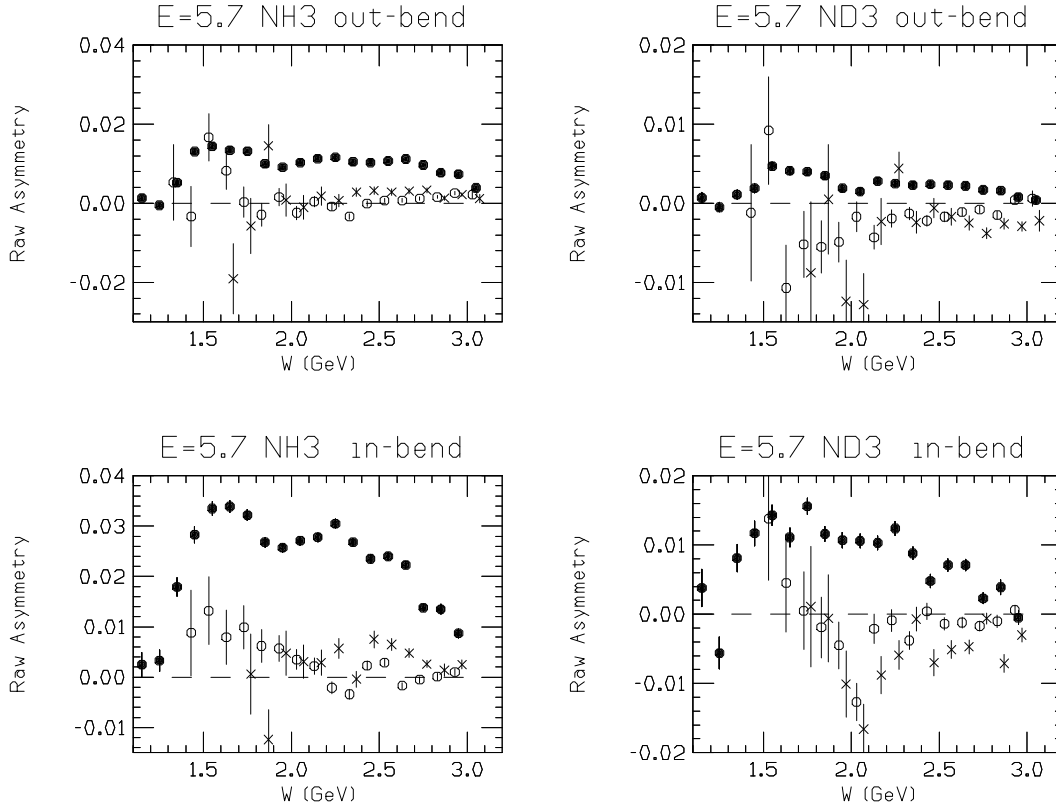


Figure 11: Same as Fig. 10, except for  $E = 5.7$  GeV.

Table 1: Estimates for  $df$  and  $dA_b/A_e$  that could be used in the evaluation of the systematic error on  $A_{corr}$ . Special treatment of the 1.6 GeV data at low  $W$  may be needed due to the large  $\pi^-$  asymmetries.

E (GeV)	target	torus	$df$	$dA_b/A_e$
1.6	NH3	inbending	$0.5f$	0.2
1.6	NH3	outbending	$0.5f$	0.2
1.6	ND3	inbending	$0.5f$	1.0
1.6	ND3	outbending	$0.5f$	1.0
5.7	NH3	inbending	$0.3f$	0.1
5.7	NH3	outbending	$0.3f$	0.2
5.7	ND3	inbending	$0.3f$	1.0
5.7	ND3	outbending	$0.3f$	1.0